Biochimica et Biophysica Acta, 598 (1980) 260—271

BBA 78702

DEUTERATED PHOSPHOLIPIDS AS RAMAN SPECTROSCOPIC PROBES OF MEMBRANE STRUCTURE

PHASE DIAGRAMS FOR THE DIPALMITOYL PHOSPHATIDYLCHOLINE(AND ITS d_{62} DERIVATIVE)-DIPALMITOYL PHOSPHATIDYLETHANOLAMINE SYSTEM

RICHARD MENDELSOHN and CHARLES C. KOCH

Department of Chemistry, Olson Laboratories, Newark College, Rutgers University, 73 Warren Street, Newark, NJ 07102 (U.S.A.)

(Received September 10th, 1979)

Key words: Membrane structure; Phase behavior; Phospholipid system; Raman spectroscopy

Summary

Raman spectroscopic techniques have been used to construct phase diagrams for the binary phospholipid systems, DPPC-d_{62}/DPPE and DPPC/DPPE (DPPC, dipalmitoyl phosphatidylcholine; DPPE, dipalmitoyl phosphatidylethanolamine). For the former, the half-width of the C-^{2}H stretching modes of the deuterated component near 2100 cm^{-1} serves as an indicator of phospholipid fluidity. The phase behavior is described semi-quantitatively using regular solution theory with the following non-ideality parameters:

$\rho_0^{(l)} = 0.75$ kcal/mol and $\rho_0^{(s)} = 1.05$ kcal/mol

The use of deuterated phospholipids as one component of a binary mixture permits direct evaluation of the conformation of a particular component in the mixture throughout the phase separation region. The approach is demonstrated with the help of a simple model correlating the half-width of the symmetric C-^{2}H stretching mode with the fraction of DPPC-d_{62} hydrocarbon chains in the liquid crystalline state.

The effect of chain perdeuteration on the phase behavior of DPPC with DPPE is evaluated by comparison of the phase diagram of the DPPC-d_{62}/DPPE system with that of DPPC-DPPE. The latter has been constructed previously from both probe and calorimetric techniques, and is created from the Raman spectroscopic data using the I(1130/1100) ratio to characterize the *trans-gauche* population ratio in non-deuterated hydrocarbon chains. A reasonable

Abbreviations used: DPPC, dipalmitoyl phosphatidylcholine; DPPE, dipalmitoyl phosphatidylethanolamine.

fit to the phase behavior is obtained using:

$\rho_0^{(l)} = 0.85$ kcal/mol and $\rho_0^{(s)} = 0.90$ kcal/mol

The similarities of the non-ideality parameters in the two phase diagrams indicate that the effect of perdeuteration on the phase behavior of DPPC is not extensive. The use of deuterated phospholipids as essentially unperturbed components of a model membrane system is justified.

Introduction

Binary phospholipid mixtures constitute the simplest model systems which possess some of the phase characteristics shown by biological membranes. Accordingly, a variety of physical techniques have been used to construct phase diagrams for such mixtures. Two general approaches have been successful in this regard. The first involves calorimetric measurements which yield direct determination of the phase diagrams, but allow no detailed molecular interpretation of the hydrocarbon chain conformation [1—4]. The other approach involves insertion of probe molecules for a particular spectroscopic technique such as 2,2,6,6-tetramethylpiperidine-*N*-oxyl spin labels for ESR spectroscopy [5], or chlorphyll *a* and parinaric acid for fluorescence spectroscopy [6,7] into a model membrane system. The properties of the probe molecule are then used to indirectly monitor changes in phospholipid conformation. In addition, the particular spectroscopic parameter used to characterize phase behavior can often be correlated with particular aspects of phospholipid motion or order in the bilayer. Drawbacks to the use of probe molecules include possible perturbation of the phase behavior by the probe and possible non-random insertion of the probe into regions of particular physical order or chemical structure in a complex lipid system.

The use of Raman spectroscopy to monitor phospholipid fluidity in one-component phospholipid systems is well documented [8—10]. The method does not require the use of a probe molecule, since the set of vibrational frequencies for gel phase phospholipid hydrocarbons is substantially different from that of the liquid crystal phase, so that Raman spectral data can provide insights into both the thermodynamics [11,12] and dynamics [10] of phospholipid phase behavior. Recent extensions of the method to binary phospholipid mixtures have been reported from this laboratory [13,14]. It has been shown that binary phospholipid mixtures where one component is deuterated offer two unique advantages for the study of phase behavior by Raman spectroscopic methods, namely:

(1) It is possible to directly monitor the conformation of a single component in the mixture, since the effect of deuterating the phospholipid hydrocarbon chains is to place the frequency of the conformation-sensitive C-^{2}H stretching vibrations at 2100 cm^{-1} in a spectral region free from interference from the non-deuterated chains.

(2) The C-H stretching vibrations of the non-deuterated component respond to changes in lateral interactions between phospholipid molecules and can directly monitor lateral phase separations in binary systems.

The current work addresses three aspects of the use of deuterated phospholipids in Raman spectroscopic studies of their phase behavior:

(1) The feasibility of phase diagram construction is demonstrated for the DPPC(and its d_{62} derivative)-DPPE system.

(2) The use of the Raman approach to evaluate the conformation of each component in a binary phospholipid mixture throughout the phase separation region is illustrated with the help of a simple model which correlates the observed C-^{2}H line-widths of the deuterated chains with the extent of chain melting.

(3) The effect of chain perdeuteration of the DPPC component on the phase behavior is evaluated by comparison of the phase diagram for DPPC/DPPE with that of DPPC-d_{62}/DPPE using regular solution theory as a semi-quantitative model for the phase behavior.

Materials and Methods

Phospholipids

DPPE and DPPC were obtained from Sigma Chemical Co., and chain-perdeuterated DPPC-d_{62} was obtained from Serdary Research Laboratories, London, Ontario, Canada. The phospholipids were passed through a Sephadex LH-20 column (either ethanol at 37°C or $CHCl_3/CH_3OH$, 1 : 1, were the solvents), as necessary, for purification. All phospholipids showed a single spot with the appropriate R_F value [15] by thin-layer chromatography ($CHCl_3/CH_3OH/H_2O$, 65 : 25 : 4, v/v/v) with I_2-staining. DPPC and its d_{62} derivative showed differential-scanning calorimetry curves in good agreement with literature values for both the pre-transition and the main endotherm [16,17]. All phospholipids showed Raman spectroscopic behavior in one-component systems virtually the same as published data [12,16,17]. Binary phospholipid mixtures were prepared by solvent evaporation of the appropriate chloroform solution, a procedure sucessfully used in previous phase studies of the DPPE/DPPC system [18]. The last traces of solvent were removed by evacuation in a dessicator for at least 2 h. Water was added to the phospholipid preparation and the suspension was shaken on a vortex mixer at temperatures above that of completion of phase separation for that sample.

The resulting cream-like phospholipid suspensions were injected into the Kimex melting-point capillaries used for Raman spectroscopic studies and packed slightly in a hematocrit centrifuge. The final pH of the samples was 6.0—6.5 so that the DPPE was zwitterionic in character. Samples contained approx. 6 mg lipid and 100 mg water. Deuterated hexadecane was obtained from Mercke, Sharpe and Dohme of Canada, Ltd. Hexadecane (>99% pure) was obtained from Aldrich. All solvents were spectral grade in quality.

Raman spectroscopy

The Raman apparatus used has been described previously [13]. In typical experiments, approx. 250 mW of 4880-Å radiation from an Ar^+-laser illuminated the sample which was examined in a capillary tube in the transverse mode. Samples were thermostatically controlled in a massive block similar to that described by Thomas and Barylski [19]. Temperature calibration of the

system was accomplished from determinations of the Raman melting behavior of dimyristoyl, dipalmitoyl and distearoyl phosphatidylcholines and dipalmitoyl phosphatidylethanolamine. The observed Raman melting temperatures for the main transitions were approx. 2°C below the best available calorimetric data [4]. This discrepancy probably arises from the local heating of the samples in the laser beam. All temperatures reported in this work have been corrected by 2°C in order to compensate for this effect. Spectra were measured two to three times at each temperature with the following precisions typical for the indicated measured parameters: full-width at half-maximum for the symmetric C-^{2}H stretching vibration near 2100 cm^{-1} ± 1.5 cm^{-1}; I(1130/1100) intensity ratio of the C-C stretching vibrations, 4—5% of the measured value; and I(2880/2850) intensity ratio of the C-H stretching modes, 2—3% of the measured value. The 2100 cm^{-1} line-width measurement was accomplished in highly-reproducible fashion by drawing a baseline connecting inflection points in the spectra near 2040 and 2230 cm^{-1} and measuring the full-width at half-height, I(2880/2850) was estimated from peak height measurements by drawing a baseline connecting inflection points near 2800 cm^{-1} and 3020 cm^{-1}, while I(1130/1100) was estimated again from peak height measurements above a baseline drawn between inflection points at 1000 and 1190 cm^{-1}.

Results and Discussion

Conformation dependence of the C-^{2}H line-width

Previous studies from this laboratory [14] have shown that the line-width of the symmetric C-^{2}H stretching vibrations near 2100 cm^{-1} in deuterated hydrocarbon chains increases significantly during the phospholipid gel-to-liquid crystal phase transition. It is necessary to determine those aspects of phospholipid structure which are responsible for the observed temperature dependence of the C-^{2}H line-width, since various features may be involved. For example, the C-H stretching vibrations of non-deuterated hydrocarbon chains respond both to changes in the *trans-gauche* population ratio of methylene segments and to alteration in interchain lateral packing. Gaber and Peticolas [10] have demonstrated the use of an isotopic dilution experiment to isolate changes due to *gauche* rotamer formation from those due to interchain effects. This procedure is carried out at constant temperature so that the *trans-gauche* population ratio is invariant. The results for the isotopic dilution of hexadecane in a matrix of perdeuterated hexadecane for two parameters used to characterize Raman spectra of phospholipids are shown in Fig. 1. The I(2880/2850) intensity ratio used to evaluate the C-H stretching region shows a monotonic decrease from 2.10 at 100% hexadecane/0% deuterated hexadecane to 1.42 at 10% hexadecane/90% deuterated hexadecane. The chain conformation throughout was all-*trans* as the samples were in the solid state. Our results are in good accord with those of Gaber and Peticolas [10]. The observed variation in I(2880/2850) arises from differences in interchain vibrational interaction between $C_{16}H_{34}/C_{16}H_{34}$ and $C_{16}H_{34}/C_{16}{}^2H_{34}$. Snyder et al. [20] have considered the quantitative aspects of this effect.

In contrast to the behavior of I(2880/2850), the line-width of the symmetric C-^{2}H stretching vibration at 2100 cm^{-1} does not respond significantly to altera-

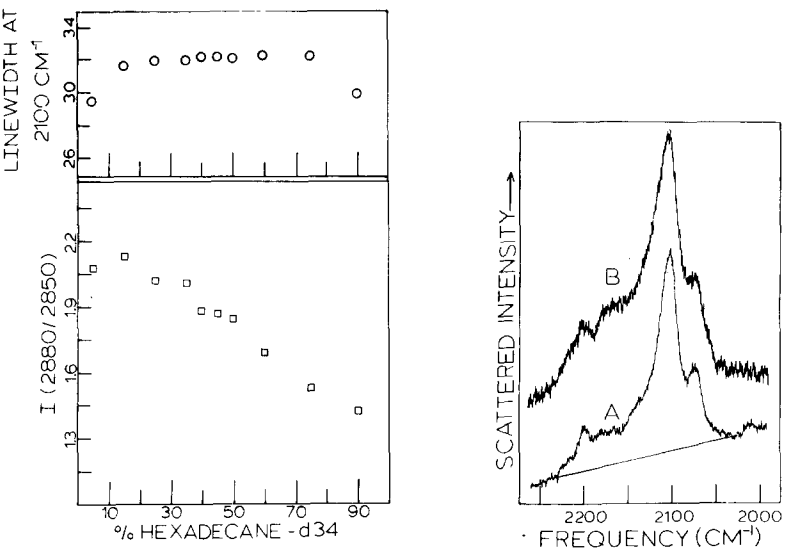

Fig. 1. Results of isotopic dilution experiments in which hexadecane was diluted to varying extents in a maxtrix of hexadecane-d_{34}. The variation of two Raman parameters as a function of percentage per-deuterated hexadecane is shown. Samples were maintained at 10° C so that the hydrocarbon chains are in the all-*trans* conformation.

Fig. 2. Typical Raman spectroscopic data for the C-^{2}H stretching vibration region (2050—2250 cm^{-1}). The sample composition is DPPC-d_{62}, 83 mol%; DPPE, 17 mol%. Temperatures at which the spectra were obtained: A 18° C, B 58° C. Typical spectral conditions: excitation frequency, 4880 Å; power, 250 mW; time constant, 5 s, slit-width, approx. 6 cm^{-1}; scan speed, 0.25 cm^{-1}/s. The baseline in A is selected to connect the inflection points in the spectra at approx. 2040 and 2230 cm^{-1}.

tions in interchain vibrational coupling. The approximate range of variation in this parameter during a phospholipid phase transition is 28 cm^{-1} (gel phase) to 48 cm^{-1} (liquid crystalline state). In the matrix isolation study (Fig. 1), the ratio is constant at approx. 32 cm^{-1} except at high dilutions (both high and low $C_{16}{}^2H_{34}$ mole fractions) where a slight decrease of approx. 2 cm^{-1} is noted. It is therefore clear that at least 90% of the observed sensitivity of the C-^{2}H line-width to melting of hydrocarbon chains and phase transitions arises from *gauche* rotamer formation. A simple model correlating the observed line-width with the fraction of chains in the liquid crystalline state is discussed in the following section.

Construction of the phase diagram for DPPC-d_{62}/DPPE

Typical Raman spectra for the C-^{2}H stretching vibration region (1950—2200 cm^{-1}) for the DPPC-d_{62}/DPPE system are shown in Fig. 2. As the temperature is increased, a significant increase in the line-width at 2100 cm^{-1} is observed. The detailed temperature-induced variation in the line-width at various mole fractions of DPPC-d_{62} is plotted in Fig. 3. The observed sigmoidal variations in the plots are indicative of phase separation processes in the binary system [14]. Onset and completion temperatures were estimated from the melting curves as shown in Fig. 3 and are tabulated in Table I. The phase diagram as determined

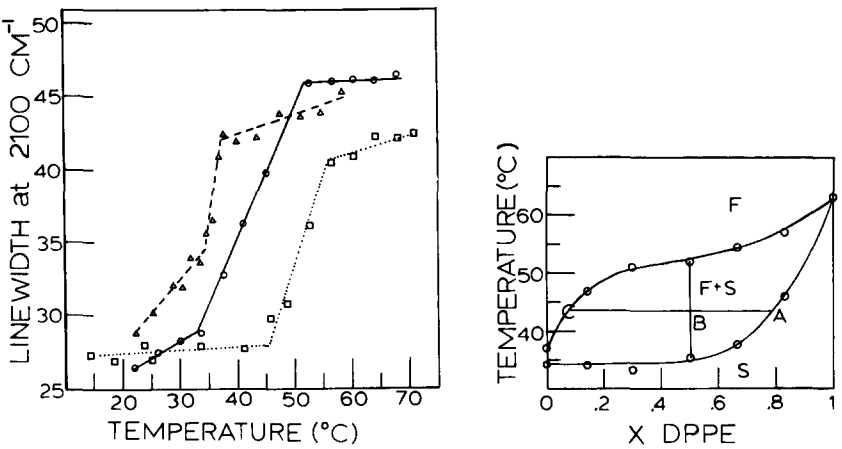

Fig. 3. Temperature-induced variation in the C-^{2}H line-width for various samples containing DPPC-d_{62} and DPPE. 100% DPPC-d_{62}, △- - - - -△; 66 mol% DPPC-d_{62}, ○———○; 16 mol/ DPPC-d_{62}, □· · · · ·□. Data points were obtained 2—4 times at each temperature. Typical standard deviations: ±1.5 cm^{-1} in the C-^{2}H line-width. Extrapolation procedures are used, as shown by the straight lines in the figure, to determine onset and completion of melting.

Fig. 4. Phase diagram for DPPC-d_{62}/DPPE determined from Raman spectroscopic data. The onset and completion temperatures for phase separation are extrapolated from data such as shown in Fig. 3. S indicates gel state phospholipid, F indicates liquid crystal lipid. See Eqn. 2 for a discussion of the use of the tie-line ABC.

from Raman spectroscopic data * from the set of onset and completion temperatures is shown in Fig. 4. The point for pure DPPE (no deuterated phospholipid present) is taken from Raman C-C data for that system.

In order to utilize the measured variation of the C-^{2}H line-width to estimate the extent of melting of each component in the binary mixture, the following protocol was adopted: (i) it was assumed that the line-shapes of the symmetric C-^{2}H stretching modes of both gel phase and liquid crystalline phospholipid were Gaussian with half-widths 28 and 48 cm^{-1}, respectively; (ii) it was further assumed that at intermediate line-widths (two phase region) the observed width comes from a weighted linear combination of gel and liquid crystal phase line-widths. The resulting band-shape is not necessarily symmetric about the peak position, since the gel phase peak appears at 2103 cm^{-1} and the liquid crystal phase peak at 2106 cm^{-1}. The intensity across the C-^{2}H band is described as:

$$I(\nu) = \frac{0.76\ Y}{\sqrt{2\pi}\ \sigma_l} \cdot \exp \frac{(\nu - 2106)^2}{2\sigma_l^2} + \frac{(1-Y)}{\sqrt{2\pi}\ \sigma_s} \cdot \exp \frac{(\nu - 2103)^2}{2\sigma_s^2} \qquad (1)$$

where Y = % DPPC-d_{62} in the liquid crystalline state and $I(\nu)$ = intensity at frequency ν. It can be shown that the relationship between σ (the square root of the variance) and the line-width (full width at half-height) is σ = line-width/$(8 \ln 2)^{1/2}$. For the liquid crystalline phospholipid, $\sigma_l = 48/(8 \ln 2)^{1/2} = 20.4$

* The uncertainties in the onset and completion temperatures are approx. 1—2°C. Higher accuracy could be obtained by acquisition of Raman data at reduced temperature intervals, but the extensive data collection required for this is not feasible with our current apparatus.

TABLE I

PARAMETERS FOR PHASE DIAGRAM CONSTRUCTION

System	Components	ΔH (kcal/mol)	T_m (°C)	$\rho_0^{(l)}$ (kcal/mol)	$\rho_0^{(s)}$ (kcal/mol)
DPPC/DPPE	DPPC	8.7 [a]	41.4 [a]	0.85	0.90
	DPPE	8.0 [b]	63 [b]		
DPPC-d_{62}/DPPE	DPPC-d_{62}	10.9 [c]	34 [d]	0.75	1.05
	DPPE	8.0	63		

[a] Ref. 4.
[b] Ref. 23.
[c] Dr. B. Gaber (private communication).
[d] From the onset temperature in the Raman melting data from the current work.

cm^{-1}. Similarly, for the gel phase, $\sigma_s = 11.9\ cm^{-1}$. The factor, 0.76, is the measured intensity ratio of the symmetric C-^{2}H stretching modes in the liquid crystalline and gel phases. From Eqn. 1, for each value of % deuterated phospholipid in the liquid crystalline state, the two frequencies at which the intensity is half the maximum value were calculated. The difference in the frequencies, which represents the measured half-width, is plotted in Fig. 5 as a function of % deuterated phospholipid in the liquid crystalline state.

Given the % deuterated phospholipid at any point in the phase separation region, it is possible to estimate the extent of non-deuterated lipid melting from the tie-line connecting boundaries on the phase diagram and the lever rule. As shown in Fig. 4, the lever rule states that:

$$\frac{A-B}{B-C} = \frac{\text{mol liquid crystalline lipid}}{\text{mol gel phase lipid}} = \frac{n_{liquid}}{n_{solid}} = \frac{X_A(f_l^A) + (1-X_A)\cdot(f_l^B)}{X_A(1-f_l^A) + (1-X_A)\cdot(1-f_l^B)} \quad (2)$$

where X_A, f_l^A and f_l^B are the mol fraction of A in the sample, the fraction of A in the liquid state and the fraction B in the liquid state, respectively. As X_A is known for the sample, n_{liquid}/n_{solid} is known from the phase diagram and f_l^A is known from the C-^{2}H line-width/extent of melting correlation for each component throughout the phase separation region. Results for the 50 : 50 mixture are shown in Fig. 6. At all temperatures in the two-phase region, the lower-melting component, DPPC-d_{62}, has melted to a much greater extent than the DPPE, as expected. In order to assess quantitatively the reliability of the correlation between the C-^{2}H line-width and the extent of melting, the percentage of each phospholipid melted was calculated in the usual way from vertical lines connecting points C and A in Fig. 4 with the abscissa. The agreement between the mole fractions of each component in each state so obtained with the data in Fig. 6 is excellent. The advantage of the Raman approach will be realized in situations where complete phase diagrams are not available, e.g., lipid-protein systems. For example, the effect of protein on the melting of deuterated lipid will be directly measureable.

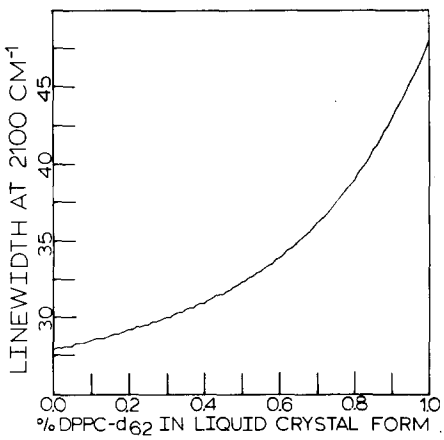

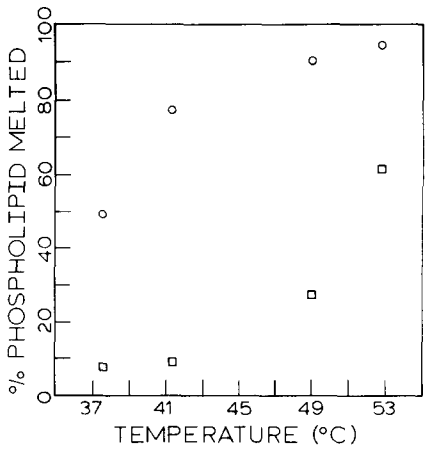

Fig. 5. Correlation of the C-^{2}H line-width with the extent of melting of DPPC-d_{62}. The curve was calculated according to Eqn. 1 in the text. The 'waviness' in the curve arises from the non-symmetric nature of the function about the point of maximum intensity.

Fig. 6. Extent of melting of each component in the binary mixture, DPPC-d_{62}/DPPE (50 : 50), calculated as per Eqn. 2 in the text. The melting of DPPC-d_{62} is given by ○; for DPPE, the extent of melting is given by □. The temperature region chosen is the two-phase region.

Comparison of DPPC-d_{62}/DPPE with DPPC/DPPE

In order to evaluate the effect of chain perdeuteration on the phase behavior of DPPC, the phase diagram for DPPC/DPPE should be compared with the data for DPPC-d_{62}/DPPE described in the previous section.

The phase diagram for DPPC/DPPE has been obtained from several types of physical measurements including calorimetry [18], spin labels [5] and chlorophyll *a* fluorescence [7]. These data are shown in Fig. 7. To demonstrate the validity of the Raman approach for phase diagram construction, it was decided to independently measure the DPPC/DPPE system. The Raman parameter of choice for the measurements is I(1130/1100). The vibrational motions involved are highly-coupled C-C stretching modes of the hydrocarbon chains which are sensitive to chain geometry [8]. Formation of *gauche* rotamers alters the coupling patterns and produces an intensity change in the C-C region of the Raman spectrum. The mode at 1130 cm^{-1} arises from C-C vibrations in all-*trans* hydrocarbon chain segments, whilst the mode near 1100 cm^{-1} arises from segments containing *gauche* rotations. The ratio, I(1130/1100), has been correlated with the number of *gauche* rotamers present in a hydrocarbon chain [10]. Although the quantitative aspects of the correlation have been questioned [21], its qualitative utility is clear. In the current experiment it is impossible to distinguish between the contributions to the spectrum from each of the non-deuterated phospholipid hydrocarbon chains. Typical Raman data for the temperature dependence of the C-C spectral region are shown in Fig. 8, while graphical data of I(1130/1100) as a function of temperature for various mole fractions are shown in Fig. 9. Onset and completion temperatures for phase separation are estimated from linear regions of the curves. The onset and completion temperatures so obtained are compared in Fig. 7 with those from other physical methods. The agreement is generally satisfactory. Of all methods

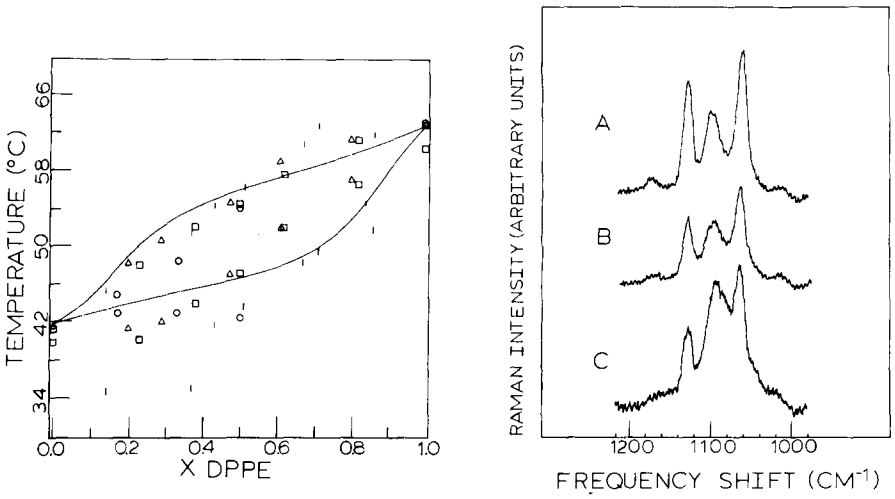

Fig. 7. Phase diagram for DPPC/DPPE calculated from several physical methods. Calorimetric data [18], |; 2,2,6,6-tetramethylpiperidine-*N*-oxyl spin labels [5], ·△; chlorophyll *a* fluorescence [7], □; and Raman spectroscopy (current work), ○. The solid curve is that calculated from regular solution theory with parameters, $\rho_0^{(l)} = 0.85$ and $\rho_0^{(s)} = 0.90$ kcal/mol.

Fig. 8. Typical Raman data for the C-C spectral region in binary phospholipid mixtures of DPPC/DPPE. The sample composition is DPPC, 83% and DPPE, 17%. Temperatures for the three traces are A 19, B 41 and C 45°C. Spectral conditions as in Fig. 2. The feature near 1130 cm^{-1} is characteristic of chain segments in the all-*trans* conformation, whilst the feature near 1100 cm^{-1} arises from chain segments containing *gauche* rotations.

used to monitor the phase behavior, only the calorimetric data (Fig. 7) show the minimum at low mole fractions of DPPE. This suggests some as yet unidentified error in the calorimetric measurements. Onset and completion temperatures in samples at high DPPE mole fractions could not be estimated

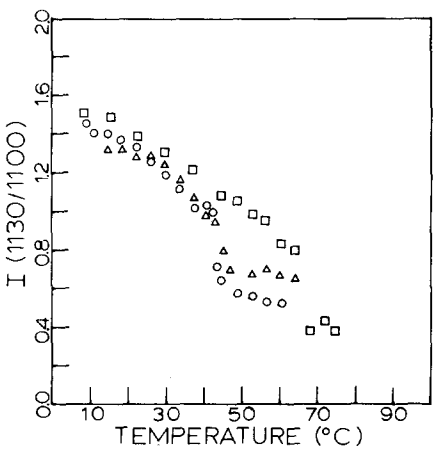

Fig. 9. Variation of $I(1130/1100)$ with temperature for various samples of DPPC/DPPE binary mixtures. 83% DPPC, ○; 67% DPPC, △; and 0% DPPC, □. At mole fractions DPPC between 0.1 and 0.4, rhe range of change in $I(1130/1100)$ during the phase separation is such that determination of the onset and completion temperatures in an unambiguous way is not possible.

from Raman spectroscopic data as the range of change in $I(1130/1100)$ during the melting process was much reduced from samples at high DPPC levels. The origin of this effect may be related to non-bilayer structures for samples with high mole fractions of DPPE.

In order to examine the effect of deuteration on the phase behavior of DPPC, the phase diagrams were simulated using regular solution theory. As the theory and its application to lipid phase behavior have been discussed in detail elsewhere [22—24], only some of the relevant equations will be listed here.

The mathematical description of a regular solution differs from a perfect solution in that the enthalpy of mixing of the components is no longer zero but is given by:

$$\Delta H_{mix} = \rho_0 X_A X_B$$

where X_A = mole fraction of A and ρ_0 is a non-ideality parameter which characterizes the solution behavior: ρ_0 may be further interpreted as the difference of A-B pair interactions from those of A-A and B-B, i.e.

$$\rho_0 = N(2U_{A\text{-}B} - U_{A\text{-}A} - U_{B\text{-}B})$$

where N is the first coordination number and $U_{A\text{-}B}$ is the molar energy of an A-B pair with other terms defined analogously.

For systems where both solid and liquid phases form regular solutions, typical expressions for the chemical potentials of components, A and B, in the solid state are given by:

$$\mu_A^{(s)} = \mu_A^{0(s)} + RT \cdot \ln X_A^{(s)} + \rho_0^{(s)}(1 - X_A^{(s)})^2 \tag{3}$$

$$\mu_B^{(s)} = \mu_B^{0(s)} + RT \cdot \ln(1 - X_A^{(s)}) + \rho_0^{(s)}(X_A^{(s)})^2 \tag{4}$$

where $\mu_A^{(s)}$ = chemical potential of component A in the solid solution, $\mu_A^{0(s)}$ = chemical potential of pure A in the solid state and $X_A^{(s)}$ = mole fraction of A in the solid phase. Equations totally analogous to Eqns. 3 and 4 above hold for the liquid phase.

The regular solution is thus characterized by non-ideality parameters, $\rho_0^{(s)}$ and $\rho_0^{(l)}$, for the solid and liquid phases, respectively. The conditions for equilibrium in the two-phase region impose the following constraints:

$$\mu_A^{(s)} = \mu_A^{(l)} \quad \text{and} \quad \mu_B^{(s)} = \mu_B^{(l)} \tag{5}$$

The following transcendental equations result:

$$\ln \frac{X_A^{(l)}}{X_A^{(s)}} + \frac{\rho_0^{(l)}(1 - X_A^{(l)})^2 - \rho_0^{(s)}(1 - X_A^{(s)})^2}{RT} = \frac{-\Delta H_A}{R}\left(\frac{1}{T} - \frac{1}{T_A}\right) \tag{6}$$

$$\ln \frac{(1 - X_A^{(l)})}{(1 - X_A^{(s)})} + \frac{\rho_0^{(l)}(X_A^{(l)})^2 - \rho_0^{(s)}(X_A^{(s)})^2}{RT} = \frac{-\Delta H_B}{R}\left(\frac{1}{T} - \frac{1}{T_B}\right) \tag{7}$$

where ΔH_A and ΔH_B = enthalpy of melting of pure A and B at their respective melting temperatures, T_A and T_B.

Eqns. 6 and 7 may be solved iteratively such that for a chosen value of T, the mole fractions of A and B in the solid and liquid phases may be obtained. The variables are considered to be ρ_0^l and ρ_0^s which may be adjusted to fit the

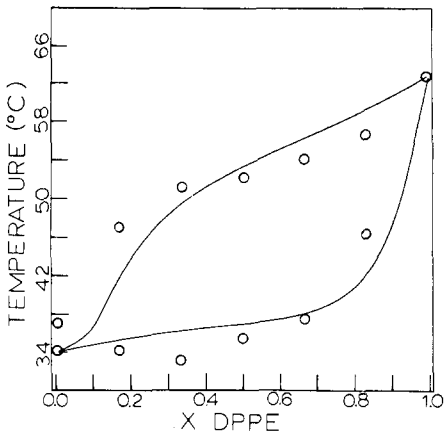

Fig. 10. Experimental (○) and calculated (———) phase diagram for the DPPC-d_{62}/DPPE binary mixture. Parameters used for the calculated curve according to regular solution theory are listed in Table I.

experimentally-determined phase diagram. Computer programs were written to carry out the iterative solution.

The parameters used to generate the phase diagrams for both DPPC-d_{62}/DPPE and DPPC/DPPE are shown in Table I. The calculated and experimental phase diagrams are given in Figs. 10 and 7. In view of the uncertainty of the experimental phase diagram for DPPC/DPPE (Fig. 7), no rigorous method for obtaining 'a best theoretical fit' to the data was tried. Computer simulations showed, however, that any variation in the non-ideality parameters by more than 200—300 cal produces a curve that lies much further away from the experimental points.

In view of the uncertainties in the experimental data and the sensitivity in the shape of the phase diagram to any variation in ρ values of more than 200—300 cal, the differences in the non-ideality parameters for the two binary systems studied are considered to be relatively insignificant. This suggests that chain perdeuteration of DPPC does not greatly alter its interactions with DPPE. The differences in the phase diagrams must be traced to differences in ΔH of melting and in the melting temperature for DPPC-d_{62} compared with DPPC.

Conclusions

The utility of deuterated phospholipids as one component of binary mixtures in Raman spectroscopic experiments is shown in the current work. Phase diagrams may be constructed using the C-^{2}H line-width near 2100 cm^{-1} as a probe of hydrocarbon chain melting. In addition, the extent of fluidization in each component throughout the phase separation region is determined both in the usual fashion [24] and from a combination of tie-lines in the Raman spectrum and the measured C-^{2}H line-width. Excellent agreement between the two approaches is seen, suggesting the possible utility of the Raman approach in the study of lipid-protein systems where complete phase diagram construction will be difficult. Currently under investigation are systems in which membrane proteins have been inserted into one- and two-component phospholipid systems. It

should be possible to deduce whether the proteins preferentially partition into particular regions of physical order or chemical structure. In addition, it may be possible to monitor the kinetics of boundary layer lipid-bulk lipid exchange in reconstituted systems. The time course of the Raman experiment will limit useful observation to a time domain of exchange with a half-life of approx. 5 min or longer.

Finally, the current work demonstrates that deuterated phospholipids have phase properties in lipid mixtures that resemble those of their non-deuterated counterparts. However, a drawback for the general applicability of the Raman technique in phase diagram construction is the extensive and time-consuming nature of the data collection required. 250—300 Raman spectra (at 15—30 min per spectrum) are required to generate a phase diagram for a two-component system. Obviously, to extend the approach to three-component systems in any meaningful way would require more advanced technological schemes for data collection. Use of vidicon techniques and computer methods for data reduction will alleviate some of the problems.

Acknowledgements

We are grateful to the donors of the Petroleum Research Fund, administered by the American Chemical Society, for support of this research through Grant No. 9894-G6 to R.M. In addition, we are indebted to Dr. Bruce Gaber for generously allowing use of his results on the enthalpy of melting for DPPC-d_{62} prior to publication.

References

1 Phillips, M.C., Ladbrooke, B.D. and Chapman, D. (1970) Biochim. Biophys. Acta 196, 35—44
2 Phillips, M.C. (1972) Prog. Surf. Membrane Sci. 5, 139—221
3 Chapman, D., Urbina, J. and Keough, K.M. (1974) J. Biol. Chem. 249, 2512—2521
4 Mabrey, S. and Sturtevant, J.M. (1976) Proc. Natl. Acad. Sci. U.S.A. 73, 3862—3866
5 Shimshick, E.J. and McConnell, H.M. (1973) Biochemistry 12, 2351—2360
6 Sklar, L.A., Hudson, B. and Simoni, R.P. (1977) Biochemistry 16, 819—828
7 Lee, A.G. (1976) Biochemistry 14, 4397—4402
8 Lippert, J.L. and Peticolas, W.L. (1971) Proc. Natl. Acad. Sci. U.S.A. 68, 1572—1576
9 Mendelsohn, R., Sunder, S. and Bernstein, H.J. (1975) Biochim. Biophys. Acta 413, 329—340
10 Gaber, B.P. and Peticolas, W.L. (1977) Biochim. Biophys. Acta 465, 260—274
11 Yellin, N. and Levin, I.W. (1977) Biochim. Biophys. Acta 468, 490—494
12 Yellin, N. and Levin, I.W. (1977) Biochim. Biophys. Acta 489, 177—190
13 Mendelsohn, R. and Maisano, J. (1978) Biochim. Biophys. Acta 506, 192—201
14 Mendelsohn, R. and Taraschi, T. (1978) Biochemistry 17, 3944—3949
15 Kates, M., Techniques of Lipidology: Laboratory Techniques in Biochemistry and Molecular Biology (Work, T.S. and Work, E., eds.), North-Holland, Amsterdam
16 Gaber, B.P., Yager, P. and Peticolas, W.L. (1978) Biophys. J. 21, 161—176
17 Gaber, B.P., Yager, P. and Peticolas, W.L. (1978) Biophys. J. 22, 191—208
18 Blume, A. and Ackerman, T. (1974) FEBS Lett. 43, 71—74
19 Thomas, G.J., Jr. and Barylski, J.R. (1970) Appl. Spectrosc. 24, 463—464
20 Snyder, R.G., Hsu, S.L. and Krimm, S. (1977) Spectrochim. Acta 34A, 395—406
21 Karvaly, B. and Loshchilova, E. (1977) Biochim. Biophys. Acta 470, 492—496
22 Pelton, A.D. and Thompson, W.T. (1975) Prog. Solid State Chem. 10, 119—155
23 Lee, A.G. (1977) Biochim. Biophys. Acta 472, 237—281
24 Lee, A.G. (1977) Biochim. Biophys. Acta 472, 285—344